Comparison of Sampling Methods for Total Radiated Power Estimation from Radio Equipment Integrated with Antennas

Nozomu ISHII[†a], ***Member***

SUMMARY EIRP measurement in the direction of maximum radiation has not always been valid to estimate the radiated power from radio equipments integrated with antennas, for example, integrated radiator with antennas shaped like the notebook-sized PC. Therefore, it is recommended that total radiated power (TRP) from equipment under test (EUT) should be estimated by integrating measured EIRPs on the whole surface of the unit sphere. In this paper, a conventional and some novel sampling methods for the TRP estimation, which were proposed to reduce the number of measurement points, are examined by using a measured EIRP data set and compared with each other. For a simulated radio equipment shaped like a notebook-sized PC, it is found that the equi-area and generalized spiral points methods are superior to the equi-angle method in terms of reducing the number of the measurement points and orthogonal three planes method is another candidate in terms of saving measurement time unless the pattern radiated from EUT is not so complicated.
key words: *total radiated power, equi-angle method, orthogonal three planes method, equi-area method, generalized spiral points method*

1. Introduction

Miniaturization of radio equipments such as mobile phone, WLAN terminal and integration of the antennas into their enclosures have become essential in the modern design-centric development. Until now, the radio equipments can be tested separately from the antenna, however, the interaction between the circuit and enclosure as well as human body remarkably affects upon the radiation pattern so that it is impossible to ignore a serious case that the radiated power from the equipment could not always be estimated by using the value of the maximum EIRP, which is conventionally applied to the measurement of the radiated power from the equipment [1]–[3]. Against this background, in 2003, CTIA (Cellular Telecommunications & Internet Association) proposed some methods of measurement for radiated power and receiver performance. In the document [1], it is recommended that the radiation characteristics should be estimated in the real operative state. Generally the maximum EIRP cannot always indicate the performance of the equipment under test (EUT) in the real operative state. Therefore, the document describes that the total radiation power (TRP) from the equipment should be measured to estimate the transmitter performance of the equipment.

As shown in Fig. 1, a radio equipment is centered at the origin of the spherical coordinate system (r, θ, ϕ). EIRP
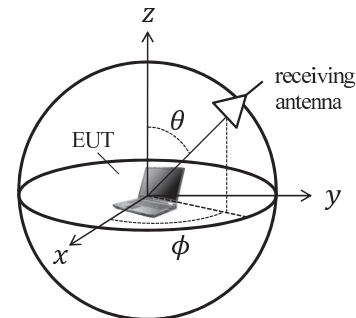
Fig. 1 EUT located in the spherical coordinate system (r, θ, ϕ).

of EUT, which denotes sum of EIRPs for the horizontal and vertical polarizations, i.e., $\text{EIRP}(\theta, \phi) = \text{EIRP}_\theta(\theta, \phi) + \text{EIRP}_\phi(\theta, \phi)$, can be measured on the surface of the unit sphere as a function of θ and ϕ, and TRP can be estimated by integrating EIRPs on the same surface as

$$\text{TRP} = \frac{1}{4\pi} \int_0^{2\pi} \int_0^\pi \text{EIRP}(\theta, \phi) \sin\theta d\theta d\phi. \quad (1)$$

In measuring the EIRPs, θ and ϕ are discretely selected as $\theta_i = (i - 1)\Delta\theta = (i - 1)(\pi/N_\theta)$ and $\phi_j = (j - 1)\Delta\phi = (j - 1)(2\pi/N_\phi)$, where $\Delta\theta$ and $\Delta\phi$ are angular intervals and N_θ and N_ϕ are division numbers in the θ and ϕ directions, respectively. Also, the integers i and j are selected as $i = 1, 2, \cdots, N_\theta + 1$ and $j = 1, 2, \cdots, N_\phi$. Then, TRP can be approximated as

$$\text{TRP} \approx \frac{\pi}{2N_\theta N_\phi} \sum_{i=2}^{N_\theta} \sum_{j=1}^{N_\phi} \text{EIRP}(\theta_i, \phi_j) \sin\theta_i. \quad (2)$$

In (2), the number of sampling points is given by $N = (N_\theta - 1)N_\phi$, because $\sin\theta_i = 0$ for $i = 1$ and $N_\theta + 1$ can be ignored. In the document [1], the angular intervals should be at least less than 15°. If the division numbers are selected as $N_\theta = 12$ and $N_\phi = 24$ for $\Delta\theta = \Delta\phi = 15°$, it is required that EIRPs should be measured at 264 sampling points on the surface of the unit sphere.

There are two serious difficulties in the above equi-angle method for the TRP estimation, based on (2):

1. It requires more measurement time as the angular intervals are selected to be smaller.
2. It includes the weight of $\sin\theta$. TRP should not be dependent upon the selection of any coordinate system.

However, the weight is nearly equal to 0 near the poles of the surface of the unit sphere ($\theta \approx 0$ or π) and is nearly equal to 1 near the equator ($\theta \approx \pi/2$) so that TRP might be misestimated due to error in alignment.

To overcome the first difficulty, we should stop two dimensional scan of θ and ϕ. For example, a simple and time-saving method for the TRP estimation was proposed [5], [6]. In this method, TRP could be approximated by measuring and numerically integrating EIRPs along a few pattern cuts, and typically one of θ and ϕ is fixed and the other is changed in the pattern cuts so that the number of the sampling points can be reduced.

To overcome the second difficulty, the sampling points should be uniformly distributed on the surface of the unit sphere. Then EIRPs at these points can be measured and averaged to estimate TRP. Some methods which can allocate the sampling points uniformly on the surface of the unit sphere, for example, equi-area method and generalized spiral points method, were applied to the TRP estimation [7]–[9].

As described above, some sampling methods for the TRP estimation were proposed, however, very few references discussed the merits/demerits of each method using an EIRP data set. In [9], some methods were compared with each other using a simulated EIRP data set. In this paper, some sampling methods for the TRP estimation are reviewed for comparison. Especially, the formulation for equi-area method derived by the author is described in detail. Then the merits/demerits of these methods for the TRP estimation are discussed by using a measured EIRP data set [10].

2. Sampling Methods for TRP Estimation

2.1 Equi-Angle Method

Based on (2), EIRPs are measured at θ_i and ϕ_j on the surface of unit sphere at angular intervals of $\Delta\theta$ and $\Delta\phi$. This sampling method or equi-angle method is a conventional method for the TRP estimation as described in the documents [1], [2] and textbook [4].

2.2 Orthogonal Three Planes Method

For short and half-wavelength dipole antennas, the average of the gain over the whole surface of the unit sphere is nearly equal to the average of the gain in three planes, for example, xy-plane ($\theta = \pi/2$, ϕ: variable), xz-plane (θ: variable, $\phi = 0$ or π) and yz-plane (θ: variable, $\phi = \pi/2$ or $3\pi/2$) [6]. In the orthogonal three planes method based on this fact, TRP is assumed to correspond to the average of $\langle\text{EIRP}\rangle_{xy}$, $\langle\text{EIRP}\rangle_{xz}$ and $\langle\text{EIRP}\rangle_{yz}$, which mean the averages of EIRP in the xy, xz and yz-plane, respectively [5]. Thus, TRP can be estimated as

$$\text{TRP} = \frac{1}{3}\left(\langle\text{EIRP}\rangle_{xy} + \langle\text{EIRP}\rangle_{xz} + \langle\text{EIRP}\rangle_{yz}\right), \tag{3}$$

where

$$\langle\text{EIRP}\rangle_{xy} = \frac{1}{N_\phi}\sum_{j=1}^{N_\phi}\text{EIRP}(\pi/2, \phi_j), \tag{4}$$

$$\langle\text{EIRP}\rangle_{xz} = \frac{1}{2N_\theta}\sum_{i=1}^{N_\theta}\{\text{EIRP}(\theta_i, 0) + \text{EIRP}(\theta_{N_\theta-i+2}, \pi)\}, \tag{5}$$

$$\langle\text{EIRP}\rangle_{yz} = \frac{1}{2N_\theta}\sum_{i=1}^{N_\theta}\{\text{EIRP}(\theta_i, \pi/2) + \text{EIRP}(\theta_{N_\theta-i+2}, 3\pi/2)\}, \tag{6}$$

where θ_i in (5) and (6) and ϕ_j in (4) are selected as $\theta_i = (i-1)\Delta\theta = (i-1)(\pi/N_\theta)$ and $\phi_j = (j-1)\Delta\phi = (j-1)(2\pi/N_\phi)$. Also, $\Delta\theta$ and $\Delta\phi$ are angular intervals and N_θ and N_ϕ are division numbers in the θ and ϕ directions, respectively. The integers i and j are selected as $i = 1, 2, \cdots, N_\theta + 1$ and $j = 1, 2, \cdots, N_\phi$.

In practice, EIRPs are measured in only the three planes so that the number of the sampling points, $N = 4N_\theta + N_\phi - 6$, could be considerably small in comparison with the equi-angle method, for example, $N = 66$ for $\Delta\theta = \Delta\phi = 15°$. A similar sampling method by using other three planes, that is, $\phi = 0$ and π plane, $\phi = \pi/3$ and $4\pi/3$ plane and $\phi = 2\pi/3$ and $5\pi/3$ plane, was also proposed for the TRP estimation of the mobile phone [5], [11], but it will not be considered in this paper because the selected three planes are not orthogonal.

2.3 Equi-Area Method

By using the element of solid angle $d\Omega$ of a sphere, TRP given by (1) can be rewritten as

$$\text{TRP} = \frac{1}{4\pi}\iint_\Omega \text{EIRP}(\theta, \phi)d\Omega, \tag{7}$$

where Ω is solid angle of the sphere. To estimate the surface integral, the surface of the unit sphere can be partitioned into equal-area regions. If (θ_k, ϕ_k) represents a point in the k-th region, TRP can be approximated as

$$\text{TRP} \approx \frac{1}{N}\sum_{k=1}^{N}\text{EIRP}(\theta_k, \phi_k), \tag{8}$$

where N is the number of the equi-area regions.

An equi-area division algorithm used in this paper is based on the recursive algorithm for multi-dimensional spherical surface proposed by P. Leopardi [12]. Let us consider a surface of the unit sphere. Its center is located at the origin of the spherical coordinate system (r, θ, ϕ) as shown in Fig. 1. In the equi-area division algorithm, first, we must give total division number N, which determines the accuracy of the TRP estimation and the total measurement time for EIRPs at (θ_k, ϕ_k), where $k = 1, 2, \cdots, N$. Next, the division number in the θ direction, n, is determined, and then
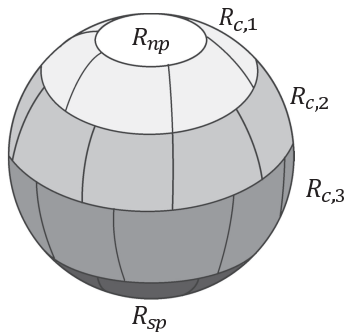
Fig. 2 An example of allocating equi-area regions on the surface of the unit sphere by equi-area division algorithm.
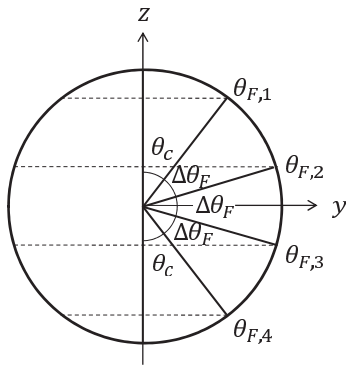

Fig. 3 The division of the collar regions in the θ direction for $n = 3$ in the yz plane.

the division number in the ϕ direction for each collar region $R_{c,i}$, m_i, is determined as all partitioned regions have equal area. A brief procedure is described as below:

1. The surface of the unit sphere is divided into two polar cap regions whose centers are located at $\theta = 0, \pi$ and several collar regions between the cap regions, as shown in Fig. 2.
2. The ranges of the cap regions R_{np}: $0 < \theta < \theta_c$ and R_{sp}: $\pi - \theta_c < \theta < \pi$ are determined.
3. The number of the collar regions, n, is determined as $n\Delta\theta_F = \pi - 2\theta_c$, where $\Delta\theta_F$ is angle which each collar region occupies in the θ direction as shown in Fig. 3.
4. The division number in each collar region $R_{c,i}$, m_i, is determined as $m_i\Delta\phi_i = 2\pi$, where $\Delta\phi_i$ is angular occupation of each equi-area region in the collar region $R_{c,i}$ in the ϕ direction.
5. The sampling point or center point for each equi-area region $(\theta_{s,i}, \phi_{s,(i,j)})$ is determined.
6. EIRP$(\theta_{s,i}, \phi_{s,(i,j)})$ are measured and averaged to estimate TRP.

The following concretely describes above procedure and derivation of the equations required to determine the equi-area regions. First, ideal area of the equi-area regions can be given by
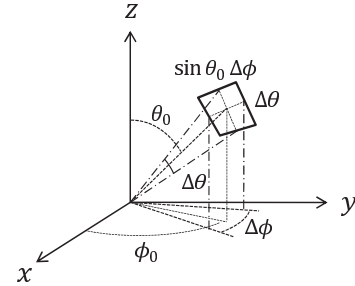

Fig. 4 An element on the surface of the unit sphere in the range of $\theta_0 - \Delta\theta/2 \le \theta \le \theta_0 + \Delta\theta/2$ and $\phi_0 - \Delta\phi/2 \le \phi \le \phi_0 + \Delta\phi/2$.

$$A_R = \frac{4\pi}{N}, \tag{9}$$

where 4π is surface area of the unit sphere and N is the number of the sampling points. The north cap region centered at the north pole, $\theta = 0$, denoted by R_{np}, is occupied from $\theta = 0$ to $\theta = \theta_c$ so that the area of R_{np} can be given by

$$A_c = \int_0^{2\pi} \int_0^{\theta_c} \sin\theta d\theta d\phi = 4\pi \sin^2\frac{\theta_c}{2}. \tag{10}$$

Similarly, the area of the south cap region centered at the south pole, $\theta = \pi$, denoted by R_{sp}, is occupied from $\theta = \pi - \theta_c$ to $\theta = \pi$ so that the area of R_{sp} can be given by A_c. By assuming that A_c is equal to A_R, θ_c can be given by

$$\theta_c = 2\sin^{-1}\sqrt{\frac{A_R}{4\pi}}. \tag{11}$$

Next, we consider the number of the collar regions, n. As shown in Fig. 4, we assume that $\Delta\theta$ denotes angular occupation of the collar region $R_{c,i}$ in the θ direction and $\Delta\phi$ denotes angular occupation of the equi-area region in the ϕ direction. If the center point of the equi-area region is set to $(1, \theta_0, \phi_0)$ in the spherical coordinate system, the area of the equi-area region can be calculated as

$$A_R = \int_{\phi_0-\Delta\phi/2}^{\phi_0+\Delta\phi/2} \int_{\theta_0-\Delta\theta/2}^{\theta_0+\Delta\theta/2} \sin\theta d\theta d\phi$$
$$= 2\sin\frac{\Delta\theta}{2}\sin\theta_0\Delta\phi \approx (\Delta\theta) \cdot (\sin\theta_0\Delta\phi). \tag{12}$$

where N is assumed to be so large that $\Delta\theta \ll 1$, $\Delta\phi \ll 1$ and $\sin(\Delta\theta/2) \approx \Delta\theta/2$. Thus, A_R is approximately equal to the area of the surface element at $(1, \theta_0, \phi_0)$ so that both $\Delta\theta$ and $\sin\theta_0\Delta\phi$ should be ideally equal to $\sqrt{A_R}$. This fact leads to the ideal angular interval for the collar region as

$$\Delta\theta_I = \sqrt{A_R}. \tag{13}$$

The collar regions occupy the surface of unit sphere except two cap regions R_{np} and R_{sp}, that is, $\theta_c \le \theta \le \pi - \theta_c$, therefore the ideal number of the collar regions is given by

$$n_I = \frac{\pi - 2\theta_c}{\Delta\theta_I}. \tag{14}$$

Since the actual number of the collar regions must be integer, it is necessary to round n_I to unit, it is given by
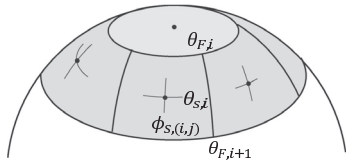
Fig. 5 An example of allocating sampling points at the center of the equi-area regions.

$$n = \text{round}(n_I). \tag{15}$$

where round() denotes round-off function. Then, the actual angular interval for the collar region $R_{c,i}$ is calculated as

$$\Delta\theta_F = \frac{n_I}{n}\Delta\theta_I = \frac{\pi - 2\theta_c}{n}. \tag{16}$$

As shown in Fig. 3, the boundaries of the collar regions are given by

$$\theta_{F,i} = \theta_c + (i - 1)\Delta\theta_F, \tag{17}$$

where $i = 1, 2, \cdots, n + 1$.

And now we consider the number of the equi-area regions in each collar region. Ideally, it can be determined by dividing the area of the collar region $R_{c,i}$ for $\theta_{F,i} \le \theta \le \theta_{F,i+1}$ by the ideal area of the equi-area region A_R. Thus, the ideal number of the equi-area region in the collar region $R_{c,i}$ is given by

$$
\begin{aligned}
y_i &= \frac{1}{A_R}\int_0^{2\pi}\int_{\theta_{F,i}}^{\theta_{F,i+1}} \sin\theta d\theta d\phi \\
&= \frac{2\pi(\cos\theta_{F,i} - \cos\theta_{F,i+1})}{A_R}.
\end{aligned} \tag{18}
$$

Since the number of the equi-area regions in the collar region $R_{c,i}$, m_i must be integer, it is determined by the following recursive equations as

$$m_i = \text{round}(y_i + a_{i-1}), \quad a_i = \sum_{j=1}^{i}(y_j - m_j), \tag{19}$$

where $a_0 = 0$ and $i = 1, 2, \cdots, n$. The actual angular interval for the collar region $R_{c,i}$ in the ϕ direction is given by

$$\Delta\phi_i = \frac{2\pi}{m_i}. \tag{20}$$

The sampling points can be allocated at the center points of the equi-area regions. The sampling angles in the θ direction can be given by

$$\theta_{s,i} = \frac{\theta_{F,i} + \theta_{F,i+1}}{2}, \tag{21}$$

for $i = 1, 2, \cdots, n$, and $\theta_{s,0} = 0$ and $\theta_{s,n+1} = 0$. If the initial angle $\phi_{\text{init},i}$ is given, the sampling angles in the ϕ direction can be given by

$$\phi_{s,(i,j)} = \phi_{\text{init},i} + j\Delta\phi_i, \tag{22}$$
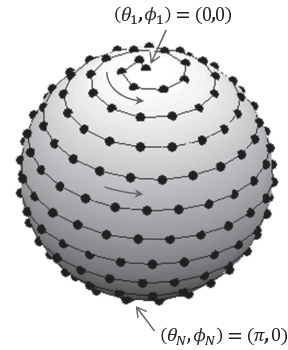

Fig. 6 An example of allocating sampling points along a sprial curve for $N = 200$.

for $j = 1, 2, \cdots, m_i$. An example of allocating the sampling points is shown in Fig. 5.

In practice, the areas of divided equi-area regions are slightly different from each other if the division number N is not so large. Therefore, we should take account of this area difference in the TRP estimation as

$$\text{TRP} = \frac{1}{4\pi}\sum_{i=0}^{n+1}\sum_{j=1}^{m_i}\text{EIRP}(\theta_{s,i}, \phi_{s,(i,j)})A_i, \tag{23}$$

where $A_i \approx \sin\theta_{s,i}\Delta\theta_F\Delta\phi_i$ denotes the area of the equi-area regions in the collar region $R_{c,i}$. If the division number N is large, A_i approaches A_R and TRP can be estimated as

$$\text{TRP} = \frac{1}{N}\sum_{i=0}^{n+1}\sum_{j=1}^{m_i}\text{EIRP}(\theta_{s,i}, \phi_{s,(i,j)}). \tag{24}$$

2.4 Generalized Spiral Points Method

As the equi-area method, the sampling points can be allocated uniformly and systematically on the surface of the unit sphere in the generalized spiral points method [13], [14]. For the number of the sampling points N, the first point can be allocated to the north pole, $(\theta_1, \phi_1) = (0, 0)$, the last point can be allocated to the south pole, $(\theta_N, \phi_N) = (\pi, 0)$, and k-th point for $k = 2, 3, \cdots, N - 1$ is allocated by following recursive relation:
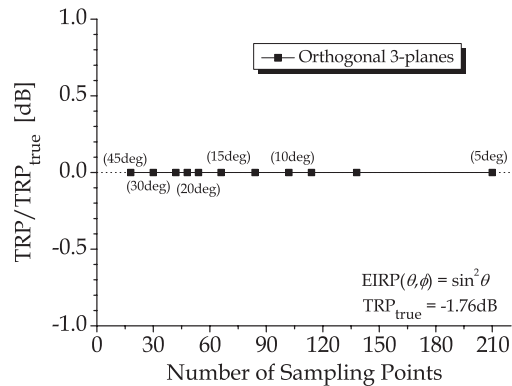
$$h_k = 1 - 2\frac{k - 1}{N - 1}, \tag{25}$$

$$\theta_k = \cos^{-1} h_k, \tag{26}$$

$$\phi_k = \phi_{k-1} + \frac{3.6}{\sqrt{N}}\frac{1}{\sqrt{1 - h_k^2}}. \tag{27}$$

Since the sampling points are allocated along a spiral curve on the surface of the unit sphere as shown in Fig. 6, they can be continuously moved by using two positioners so that saving the measurement time can be expected [9].

2.5 Estimated TRPs for Well-Known Radiation Pattern

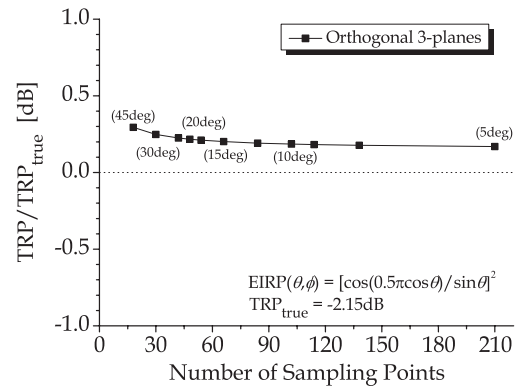To examine the validity of the above sampling methods
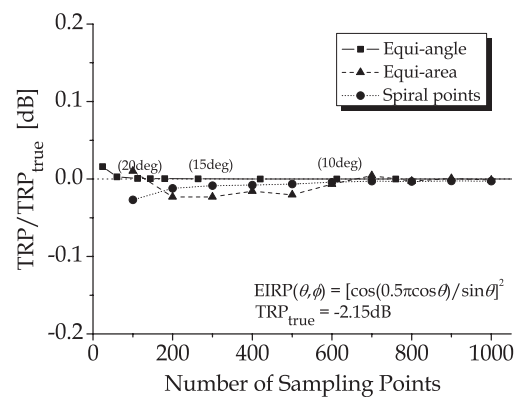
(a) Orthogonal three planes method
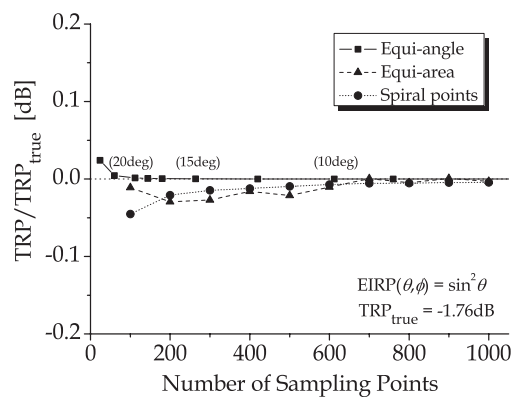
(b) Equi-angle, equi-area, and generalized spiral points methods

Fig. 7 TRPs estimated by four methods as a function of the number of the sampling points for $\mathrm{EIRP}(\theta, \phi) = \sin^2\theta$.

(a) Orthogonal three planes method

(b) Equi-angle, equi-area, and generalized spiral points methods

Fig. 8 TRPs estimated by four methods as a function of the number of the sampling points for $\mathrm{EIRP}(\theta, \phi) = [\cos(\frac{\pi}{2}\cos\theta)/\sin\theta]^2$.

for the TRP estimation, TRPs are calculated as a function of the number of sampling points, N, for well-known radiation patterns, (i) $\mathrm{EIRP} = \sin^2\theta$ and (ii) $\mathrm{EIRP} = [\cos(\frac{\pi}{2}\cos\theta)/\sin\theta]^2$, which are corresponding to the radiation patterns of the infinitesimal dipole antenna and half-wavelength dipole antenna, respectively. The true values of TRP are rigorously calculated to be $-1.76\,\mathrm{dB}$ and $-2.15\,\mathrm{dB}$ in the cases of (i) and (ii), respectively. The differences of estimated TRPs from the true TRPs are shown in Figs. 7 and 8, as a function of N, for the four sampling methods. The sampling points allocated by the sampling methods are not always coincident with measurable points. In the above calculation, the measurable points are assumed to exist at angular interval of $1°$ in the θ and ϕ directions, and are substituted for the sampling points. In practice, EIRPs at the measurable points nearest the sampling points are used to calculate TRP.

In the case of (i) $\mathrm{EIRP} = \sin^2\theta$, the convergence of the estimated TRPs is rapid as N is larger. The differences between the estimated and true TRPs are less than 0.1 dB and may be caused by sampling at not the allocated points but the measurable points for the four sampling methods. In the case of (ii) $\mathrm{EIRP} = [\cos(\frac{\pi}{2}\cos\theta)/\sin\theta]^2$, the convergence of the estimated TRPs is rapid as N is larger. The differences
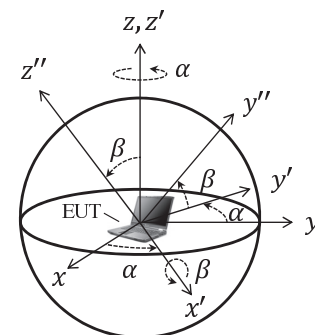

Fig. 9 Two rotations of the spherical coordinate system with angles α and β.

between the estimated and true TRPs are less than 0.1 dB and may be caused by sampling at the measurable points for the equi-angle, equi-area, and generalized spiral points methods. For the orthogonal three planes method, the differences between estimated and true TRPs is less than 0.2 dB when $N \geq 66$. However, the estimated TRP does not exactly approach to the true TRP as N is larger. This is because the sampling points are selected at the points or the directions (θ, ϕ) where the EIRP is rapidly changed. If the coordinate is rotated along the x axis with $\alpha = 0°$ and $\beta = 45°$ as shown

in Fig. 9, the TRP is estimated to be -2.18 dB at $N = 66$. Thus, the selection of the coordinate system is somewhat severe for the rapid change of the radiation pattern when the orthogonal three planes method is used.

3. Simulated Radio Equipments and Measurement Condition

3.1 EIRP Data Set of Simulated Radio Equipments

EIRPs of a simulated radio equipments shaped like a notebook sized PC were measured as a function of elevation and azimuth angles by Telecom Engineering Center (TELEC), Japan [10]. A conical cut measurement system for spherical radiation pattern had developed by TELEC. EUT was centered at the origin of the spherical coordinate system. Measured EIRPs were related to the fundamental, second and third harmonics, fundamentally operated at 2.412 GHz. The angular intervals of $\Delta\theta_{mes}$ and $\Delta\phi_{mes}$ in the θ and ϕ directions for the EIRP measurement are listed in Table 1. In this paper, it is assumed that EIRP had already measured as a function of θ and ϕ, and the procedure and calibration for the EIRP measurement will not be described.

3D patterns and pattern cuts of the EUT in the xy plane are shown in Figs. 10 and 11, respectively. The pattern at 2.412 GHz changes somewhat gradually, however the patterns at 4.824 GHz and 7.236 GHz change rapidly in part and have many nulls so that the sampling methods may not exactly integrate the EIRP over the spherical surface.

According to Ref. [10], the extended uncertainties of the EIRP measurement are estimated to be 2.29 dB, 4.85 dB, and 5.15 dB at 2.412 GHz, 4.824 GHz, and 7.236 GHz, respectively. Reference [10] reported that the main factor of the uncertainty is due to the ripple in the quiet zone of the measurement system and has a stronger effect on the uncertainty as the frequency is higher. This factor can lead to the error of the estimated TRPs obtained by the sampling methods.

3.2 Selection of Sampling Points

For the equi-area and generalized spiral points methods, the most accurate TRP can be estimated by using measured EIRPs at sampling points specified by the algorithms. Since EIRPs are sampled at angular intervals listed in Table 1, measured EIRPs do not exist at the sampling points specified by the algorithms. In this paper, it is assumed that the division number is so large, or the area of the divided regions is so small that EIRP can be replaced by measured EIRP in the divided region or at the nearest to the sampling point specified by the algorithms. Of course, as the division number is smaller, this approximation becomes worse or the uncertainty due to selecting the sampling points should be considered.

Table 1 Angular intervals in the EIRP measurement of a simulated radio equipment shaped like notebook-sized PC.

Frequency [GHz]	$\Delta\theta_{mes}$ [deg]	$\Delta\phi_{mes}$ [deg]
2.412	5	1
4.824	1	1
7.236	1	1

(a) 2.412 GHz, θ polarization

(b) 2.412 GHz, ϕ polarization

(c) 4.824 GHz, θ polarization

(d) 4.824 GHz, ϕ polarization

(e) 7.236 GHz, θ polarization

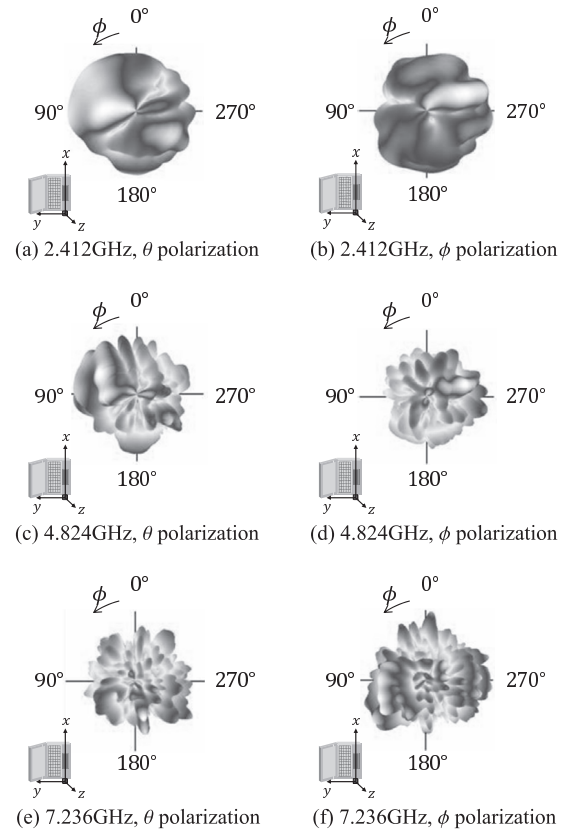(f) 7.236 GHz, ϕ polarization

Fig. 10 3D-patterns of EUT for the θ and ϕ polarizations [10].

## 4. Comparison of TRP Estimated by Various Sampling Methods

To make the following discussion clear, reference TRP level, TRP_{ref}, is defined as TRP level estimated by the equi-angle method at angular intervals of $5°$, because the differences between this reference level and estimated TRP levels at angular intervals of $\Delta\phi = 2°$ or $1°$ and $\Delta\theta = 5°$ is selected at 2.412 GHz are less than 0.02 dB.

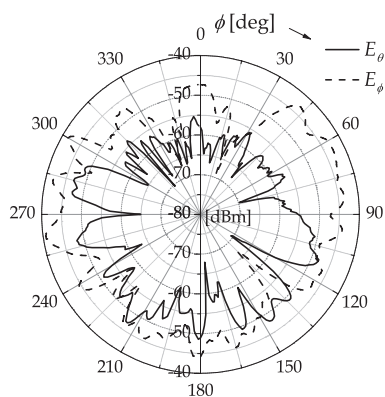### 4.1 TRP Estimated by Orthogonal Three Planes Method

Figure 12 shows TRP estimated by using the orthogonal three planes method at the frequency of (a) 2.412 GHz, (b) 4.824 GHz, and (c) 7.236 GHz, as a function of the number of the sampling points N. At 2.412 GHz, estimated TRPs tend to approach TRP_{ref} as N is larger. The differences between TRP_{ref} and estimated TRPs at angular intervals of $5°$ to $15°$ are within 0.7 dB. At 4.824 GHz and 7.236 GHz, es-
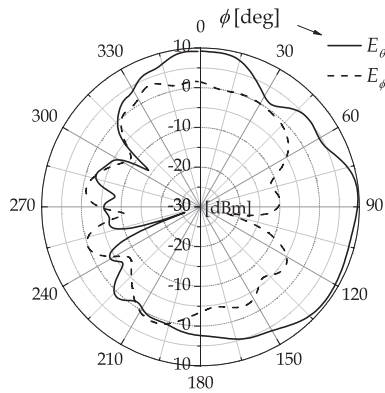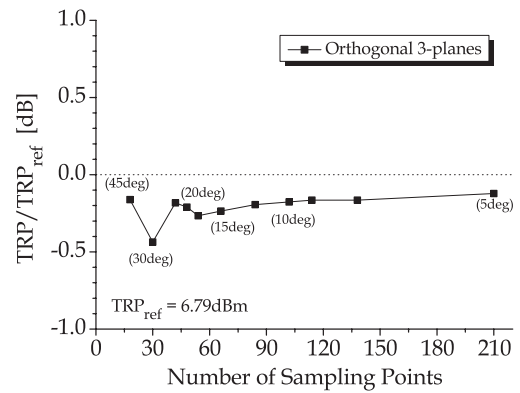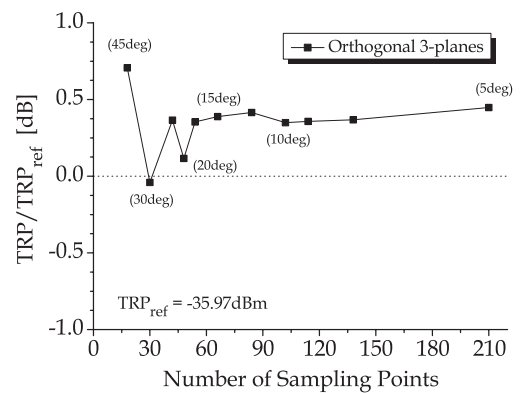
(a) 2.412GHz

(a) 2.412GHz
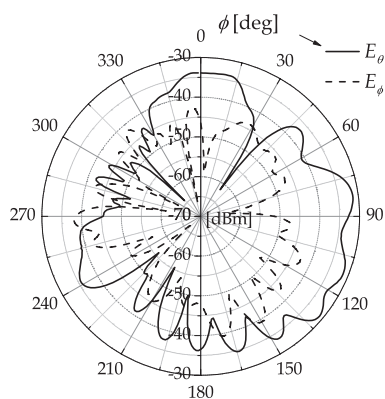
(b) 4.824GHz

(b) 4.824GHz

(c) 7.236GHz

Fig. 11   Pattern cuts of EUT in the *xy* plane [10].

(c) 7.236GHz

Fig. 12   TRPs estimated by orthogonal three planes method as a function of the number of the sampling points.
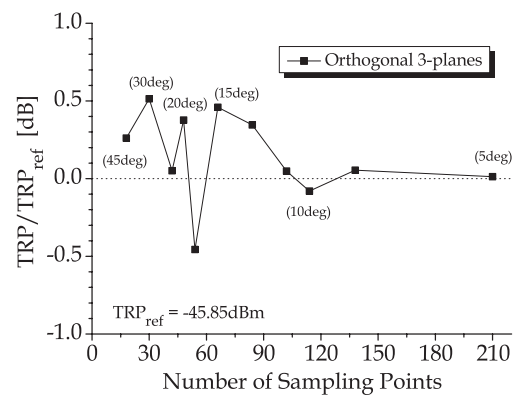
timated TRPs are nearly equal to TRP_{ref}, but do not completely converge with TRP_{ref} as N is larger. The reason why the differences are not vanished is not completely to satisfy the condition that the radiation pattern from EUT is almost omni-directional or slowly-varying as a function of θ and ϕ. In fact, EUT has complicated patterns as shown in Figs. 10 and 11 [10].

4.2   TRP Estimated by Equi-Angle, Equi-Area and Generalized Spiral Points Methods
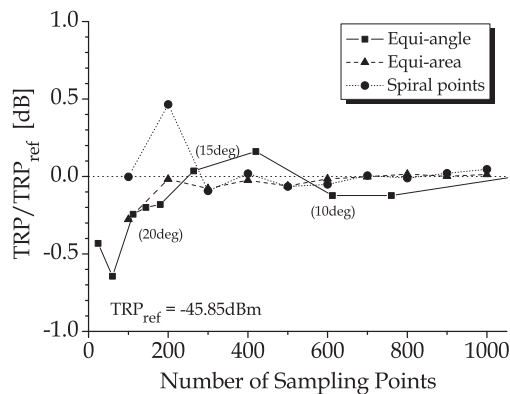
Figure 13 shows TRP estimated by using the equi-angle, equi-area, and generalized spiral points methods at the frequency of (a) 2.412 GHz, (b) 4.824 GHz, and (c) 7.236 GHz. In any methods, estimated TRP tends to converge with TRP_{ref} as the number of the sampling points N is larger. At higher frequency, the uncertainty of estimated TRP in-
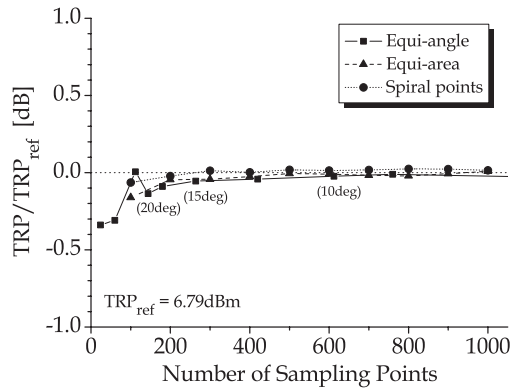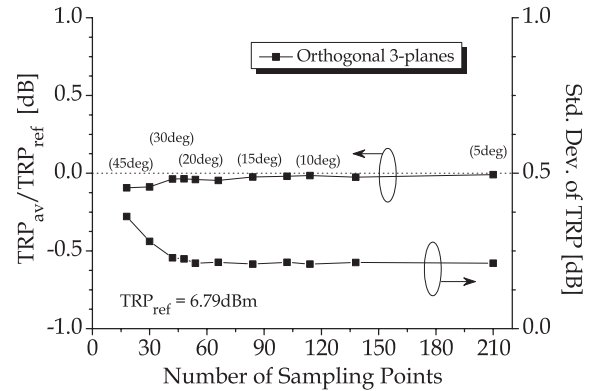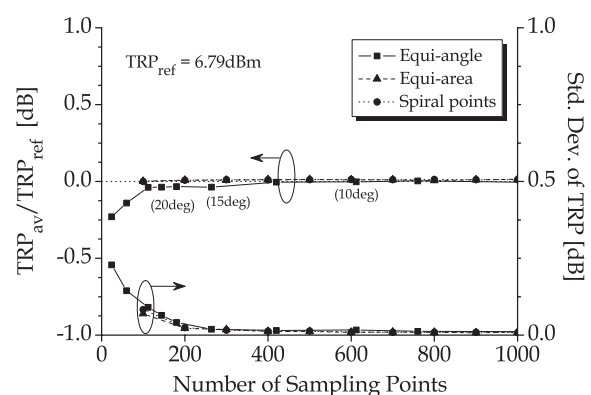
(a) 2.412GHz
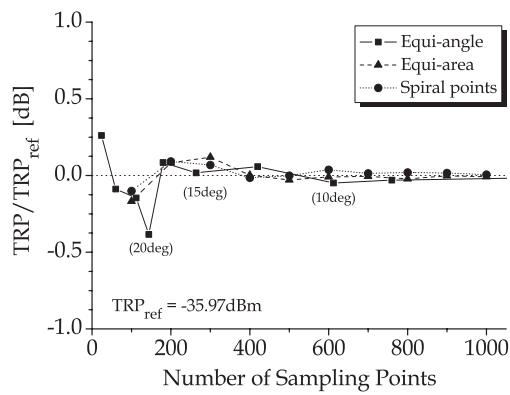
(b) 4.824GHz

(c) 7.236GHz

Fig. 13 TRPs estimated by equi-angle, equi-area, and generalized spiral points methods as a function of the number of the sampling points.

(a) Orthogonal three planes method

(b) Equi-angle, equi-area, and generalized spiral points methods

Fig. 15 Average and standard deviation of estimated TRPs at 2.412 GHz by rotating the coordinate system with the rotation angles of α and β.

creases because the radiation pattern changes rapidly as shown in Figs. 10(b), (c) and Figs. 11(b), (c) as well as the uncertainty of the measured EIRPs increases, as described in Sect. 3.1. Therefore, it is impossible simply to judge the advantage of these methods, but it is possible to read the tendency of the convergence in practical measurements.

As seen in Fig. 13, the equi-area and generalized spiral points methods tend to be able to allocate less sampling points uniformly than the equi-angle method. The differ-

ences between $\mathrm{TRP_{ref}}$ and TRPs estimated by the equi-angle method at angular intervals of 15°, which means that the number of the sampling points is given by $N = (N_\theta - 1)N_\phi = 264$, are within 0.1 dB. And the differences between $\mathrm{TRP_{ref}}$ and TRPs estimated by the equi-area and generalized spiral points methods for $N = 200$ are also within 0.1 dB with one exception, which corresponds to TRP estimated by the generalized spiral points method at 7.236 GHz. If the coordinate is rotated along the x axis with $\alpha = 0°$ and $\beta = 30°$ as shown in Fig. 9, the differences between $\mathrm{TRP_{ref}}$ and TRP estimated by the generalized spiral points method is less than 0.1 dB at $N = 200$. This is because N is not enough to estimate accurate TRP for the rapid change of the radiation pattern shown in Fig. 10(c) and Fig. 11(c).

4.3 Changes of TRP Levels due to 3D-Rotation of EUT

In this subsection, the changes of TRP levels estimated by aforementioned sampling methods are examined when EUT rotates α around the z axis shown in Fig. 9 and then rotates β around new x axis (x' axis), where α is changed from 0° to 345° at intervals of 15° and β is changed from 0° to 180° at intervals of 15°. Figure 14 shows the average and variation range of TRPs at 2.412 GHz as a function of the sec-

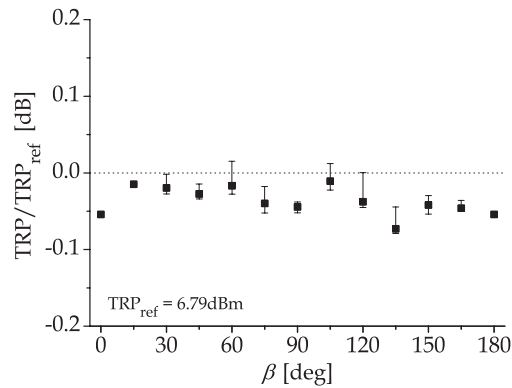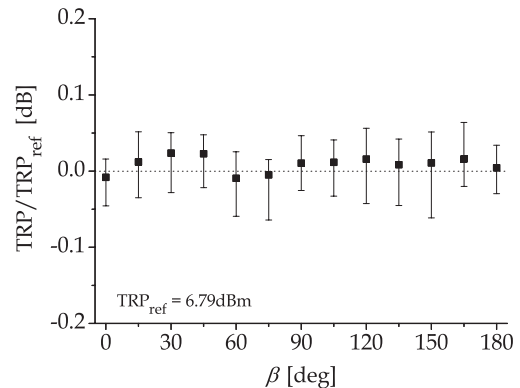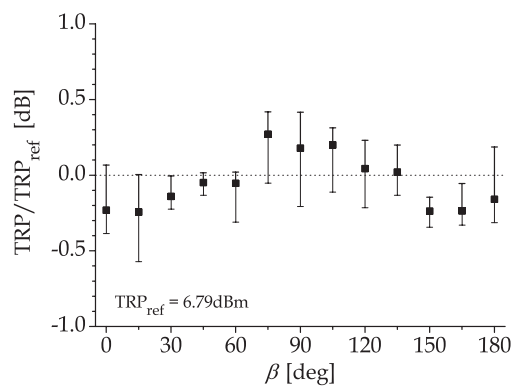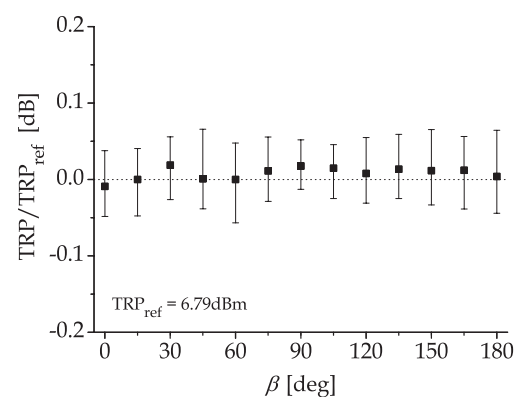(a) Equi-angle method ($N = 264$)

(b) Orthogonal three planes method ($N = 66$)

(c) Equi-area method ($N = 200$)

(d) Generalized spiral points method ($N = 200$)

Fig. 14 Estimated TRPs at 2.412 GHz by rotating the coordinate system as a function of the rotation angle, β.

ond rotation angle β, estimated by (i) equi-angle method, (ii) orthogonal three points method, (iii) equi-area method and (iv) generalized spiral points method. For example, the average value at $\beta = 30°$ shown in Fig. 14 means the average of TRPs for $\alpha = 0°, 15°, \cdots, 345°$ and $\beta = 30°$. In (i) and (ii), the angular interval is set to $15°$. In (iii) and (iv), the number of the sampling points is set to $N = 200$.

As shown in Fig. 14, TRPs estimated by (i) and (ii) depend upon β, but the differences between $\mathrm{TRP_{ref}}$ and TRPs estimated by (iii) and (iv) are less than 0.1 dB for all rotation angles of α and β. Thus, both equi-area and generalized spiral points methods may be less affected by the error in alignment of EUT.

Figure 15 shows the average and standard deviation of estimated TRPs for all α and β as a function of N. For the average, the values estimated by (iii) and (iv) are in good agreement with each other. The differences among the TRPs estimated by the four sampling method are less than 0.1 dB for $N \geq 100$. Therefore, the algorithms which can partition the surface of the unit sphere into uniform areas can be used to realize the convergence of the surface integral with less number of the sampling points than the equi-angle method. The standard deviations of (iii) and (iv) are in good agreement with that of (i) for all N and are smaller as N is larger. For example, the value of the standard deviation is 0.02 dB

for $N = 264$ of (i), 0.23 dB for $N = 66$ of (ii), and 0.02 dB for $N = 200$ of (iii) and (iv). Note that the standard deviation for the orthogonal three planes method is larger than the other sampling methods by one order of magnitude. If the standard uncertainty of 0.2 dB can be allowed, however, the orthogonal three planes method can be a candidate for the TRP estimation, which is able to save the measurement time.

5. Conculsion

In this paper, four methods for the TRP estimation are examined by using measured data of EIRP for a simulated radio equipment shaped like notebook-sized PC. The equi-area and generalized spiral points methods, where the sampling points to measure EIRPs are uniformly allocated on the surface of the unit sphere, are superior to the equi-angle method in terms of the convergence with smaller number of the sampling points, despite the uncertainties of three methods are comparable with each other. The selection of these methods for the TRP estimation as well as the number of the sampling points will be dependent upon practical requirements of measurement, for example, saving measurement time and simultaneously measuring the radiation pattern. Also, as long as the radiation pattern from the radio equipment is not

so complicated, the orthogonal three planes method can be used as a simple and time-saving method for the TRP estimation, despite the uncertainty of this method is larger than those of the other three methods by one order of magnitude.

Acknowledgment

References

[1] CTIA certification: Test plan for mobile station over the air performance — Method of measurement for radiated RF power and receiver performance, revision number 2.2.2, Dec. 2008.

[2] 3rd Generation Partnership Project, "Technical specification group radio access network: Measurements of radio performances for UMTS terminals in speech mode (release 8)," 3GPP TR 25.914 v8.0.0, 2008.

[3] Q. Chen, T. Shinohe, K. Igari, and K. Sawaya, "Measurement of power absorption by human model in the vicinity of antennas," IEICE Trans. Commum., vol.E80-B, no.5, pp.709–711, May 1997.

[4] C.A. Balanis, Antenna Theory Analysis and Design, 3rd ed., Wiley, 2005.

[5] H. Watanabe, T. Maeyama, Y. Amano, and M. Nakano, "A simple measurement technique of the total radio performances for mobile phone," IEICE Technical Report, ACT2009-11, Nov. 2009.

[6] Y. Amano, H. Ishikawa, and T. Inoue, "Mean effective gain performances of small antenna for mobile phone in 3-D and three orthogonal planes," Proc. ISAP 2008, pp.593–596, Taipei, Taiwan, Oct. 2008.

[7] S. Ullah, J.A. Flint, and R.D. Seager, "Equi-spaced-points-method (ESPM) for antenna radiation pattern (ARP) measurements with 3D-rotation," Proc. EuCAP 2007, Th2.11.6, Edinburgh, UK, Nov. 2007.

[8] N. Ishii, "Radiated power evaluation of simulated radio equipment using equi-spaced-point-method," Proc. ISAP 2009, pp.691–694, Bangkok, Thailand, Oct. 2009.

[9] M. Yoshida and H. Arai, "Total radiated power measurement using generalized spiral point sets," IEICE Technical Report, ACT2009-18, Feb. 2010.

[10] T. Watanabe, K. Nakajima, T. Shigeno, and H. Arai, "Total radiated power measurement for a portable transmitter using spherical and hemispherical scanning," IEICE Technical Report, ACT2008-13, Dec. 2008.

[11] H. Watanabe and T. Maeyama, "A simple measurement technique of the total radiated power," IEICE Trans. Commun. (Japanese Edition), vol.J93-B, no.9, pp.1292–1295, Sept. 2010.

[12] P. Leopardi, "A partition of the unit sphere into regions of equal area and small diameter," Electronic Transactions on Numerical Analysis, vol.25, pp.309–327, 2006.

[13] E.A. Rakhmanov, E.B. Saff, and Y.M. Zhou, "Minimal distance energy on sphere," Mathematical Research Letters, vol.1, pp.647–662, 1994.

[14] E.B. Saff and A.B.J. Kuijlaars, "Distributing many points on a sphere," Mathematical Research Letters, vol.19, no.1, pp.5–11, 1997.

Nozomu Ishii   was born in Sapporo, Japan, in 1966. He received the B.S., M.S., and Ph.D. degrees from Hokkaido university, Sapporo, Japan, in 1989, 1991, and 1996, respectively. In 1991, he joined the faculty of engineering at Hokkaido university. Since 1998, he has been with the faculty of engineering at Niigata university, Japan, where he is currently an associate professor of the department of biocybernetics. His current interests are in the area of small antenna, planar antenna, millimeter antenna, antenna analysis, antenna measurement, and electromagnetic compatibility. He is a member of the IEEE.